

Scientific paper

Gel-Sol Synthesis of Rutile Nanoparticles

Dejan Verhovšek,^{1,*} Maja Lešnik,¹ Nika Veronovski,¹ Zoran Samardžija,²
Kristina Žagar² and Miran Čeh²

¹ Cinkarna Celje, d.d. Inc., Kidriceva 26, SI-3001 Celje, Slovenia

² Jozef Stefan Institute, Department for Nanostructured Materials, Jamova cesta 39, SI-1000 Ljubljana, Slovenia

* Corresponding author: E-mail: dejan.verhovsek@cinkarna.si
Tel.: 00386 035 427 6114; Fax.: 00386 035 427 6116

Received: 19-12-2013

Dedicated to the memory of Prof. Dr. Marija Kosec.

Abstract

Titanium dioxide (TiO₂) rutile nanoparticles were synthesized at temperatures below 100 °C using a gel-sol process that provides control of the final particles' characteristics, such as the nanoparticle size, morphology, crystal structure and crystallinity. The synthesized rutile nanoparticles were analyzed using X-ray powder diffraction (XRD), scanning electron microscopy (SEM) and transmission electron microscopy (TEM). The results show that the gel-sol process allows control over the final nanoparticle characteristics with the proper choice of reaction parameters. The most profound influence on the nanoparticles' properties is achieved by the type and concentration of the acid used in the reaction mixture. The gel-sol synthesis resulted in anisotropic rutile nanoparticles that are 60–160 nm long, depending on the reaction parameters, and have an aspect ratio of about 5. A reaction mechanism is presented, explaining the influence of various reaction parameters on the characteristics of the TiO₂ nanoparticles.

Keywords: Rutile, nanoparticles, gel-sol synthesis

1. Introduction

A so-called nanosize-type TiO₂ has recently attracted a lot of attention because of its increased photocatalytic activity resulting from its higher specific surface. This photocatalytic activity results in the formation of superoxide and hydroxide radicals that can react with any organic material adjacent to the TiO₂ nanoparticles.¹ The ability of TiO₂ nanoparticles to produce radicals in large amounts is promising and can be usefully implemented in a variety of photocatalytic applications, e.g., in water photolysis and in anti-bactericidal applications.^{1,2} Nanosized TiO₂ can be further used as an effective UV blocking agent, as a material in novel solar cells (DSSCs) and in photo-electrochromic windows.^{3,4} This is why it is extremely important to develop suitable methods that allow the synthesis of nanosized TiO₂ with the desired physical and chemical properties.

So far very few methods are known to produce TiO₂ material with a high specific surface. Two conventional

methods for producing rutile are the high-temperature transformation from anatase^{5,6} and the direct flame oxidation of titanium tetrachloride.⁷ However, both methods produce rutile particles with a relatively low specific surface. On the other hand, a hydrothermal synthesis using suitable precursors, such as titanium tetrachloride and titanium isopropoxide, produces TiO₂ with a high specific surface area,^{8–10} but the method is expensive and technologically complicated if transferred into large-scale production. It is therefore crucial that a method is devised that would allow a cheap and simple way to produce the TiO₂ nanoparticles and at the same time enable the adjustment of the material's characteristics according to a specific application. One of the synthesis methods that allow such control is the gel-sol method. It is one of the most promising methods since it does not involve high processing temperatures or expensive equipment and enables control of the material's characteristics, depending solely on the initial reaction parameters.¹¹ The gel-sol method is able to produce monodispersed TiO₂ nanoparticles in large quan-

tities using a highly viscous gel which serves as a matrix for the growing particles to inhibit their coagulation and as a reservoir of metal ions that are released during its dissolution. Another very important advantage of the gel-sol process is the fact that at the end of the reaction the initial gel is completely converted into TiO₂ nanoparticles.

In our research we focused on studying the most important reaction parameters of the gel-sol synthesis, which include the reaction temperature, the precursor concentration and the mineral acid type and concentration, with the aim to determine their influence on the TiO₂ characteristics and to provide an insight into the mechanisms of the precursor's transformation.

2. Experimental Procedures

The precursor, i.e., sodium titanate, was provided by Cinkarna Celje Inc. and was used without any further purification. Sodium titanate used in the experiments had a mass concentration of 120 g/L (calculated as TiO₂). In each experiment 400 mL of sodium titanate was poured into a beaker and then mineral acids (HCl (37% w/w, Fluka), H₂SO₄ (98% w/w, Fluka), HNO₃ (65% w/w, Fluka) were added drop-wise until a specific mass acid concentration (in g/L) was achieved. The reaction mixture was then heated to temperatures ranging from 50 to 100 °C and stirred slowly for 3 hours. The final product was an aqueous suspension of nanoparticles. In some experiments sodium chloride (NaCl, w/w 99,5%, Merck) was also used.

To investigate the effect of temperature on the characteristics of the TiO₂ we carried out synthesis reactions

by varying only the temperature of the reaction medium, while keeping the hydrochloric acid concentration constant at 70 g/L and the TiO₂ precursor concentration constant at 120 g/L. The temperatures used during the synthesis reactions were varied from 50 to 100 °C.

When investigating the effect of supersaturation we changed the amount of the precursor in the reaction, while keeping the hydrochloric acid concentration constant at 70 g/L and the reaction temperature constant at 80 °C. The precursor concentration was varied between 60 and 180 g/L (calculated as TiO₂).

Most of the experiments were carried out using hydrochloric acid in order to determine its effect on the produced TiO₂ nanoparticles. We prepared different samples by varying the hydrochloric acid concentration, while keeping the temperature constant at 80 °C and the TiO₂ precursor concentration constant at 120 g/L. The hydrochloric acid concentrations were set to 40, 50, 60, 70, 100, 130 g/L and 160 g/L, respectively, by diluting the 37% w/w HCl.

Finally, synthesis experiments were also carried out using nitric and sulfuric acid instead of hydrochloric acid. The other reaction parameters were kept the same (80 °C, precursor concentration of 120 g/L). The nitric acid concentration was varied and was set to 70 g/L and 130 g/L, respectively, by diluting the 65% w/w HNO₃. The sulfuric acid concentration was varied and was set to 50 g/L and 100 g/L, respectively, by diluting the 98% w/w H₂SO₄.

The variations in the experimental conditions are summarized in Table 1.

The samples were characterized by using X-ray diffraction (XRD), scanning electron microscopy (SEM) and

Table 1. Summary of the experimental conditions that were varied in examining the gel-sol synthesis of TiO₂ nanoparticles using sodium titanate as the precursor.

The effect of temperature on TiO₂ nanoparticle formation – temperature variation / °C	The effect of supersaturation on TiO₂ nanoparticle formation – changing the precursor mass concentration / g/L	The effect of mineral acid concentration on TiO₂ nanoparticle formation – changing the mineral acid mass concentration / g/L		
Constant parameters: HCl mass concentration (70 g/L); sodium titanate mass concentration (120 g/L)	Constant parameters: HCl mass concentration (70 g/L); temperature (80 °C)	Constant parameters: Precursor mass concentration (120 g/L); temperature (80 °C)		
		Hydrochloric acid mass concentration / g/L	Nitric acid mass concentration / g/L	Sulfuric acid mass concentration / g/L
50	60	40	70	50
60	80	50	130	100
70	100	60		
80	120	70		
90	140	70 + NaCl (25 g/L)		
100	160	70 + NaCl (50 g/L)		
	180	70 + NaCl (100 g/L)		
	100			
	130			
	160			

transmission electron microscopy (TEM). In order to acquire TiO_2 powders for the X-ray powder diffraction (XRD) investigations, the suspensions were neutralized after the reaction, filtered, washed with distilled water and dried at 80 °C. The TiO_2 powder was pressed into a pellet and the spectra were recorded from 10° to 70° (2-theta angle) with CuK_α radiation ($\lambda = 1.5418 \text{ \AA}$) using a CubiX PRO PW 3800 instrument (PANalytical). The TiO_2 crystal structure was identified using the X'Pert Data Viewer software.

Scanning electron microscopy (SEM) (Jeol JSM-7600F, Jeol Ltd., Tokyo, Japan) and transmission electron microscopy (TEM) studies (Jeol JEM-2100, Jeol Ltd., Tokyo, Japan) were used to estimate the morphology and dimensions of the TiO_2 nanoparticles. The samples for the TEM observations were ultrasonically dispersed and placed onto lacey, carbon-coated, nickel grids.

3. Results and Discussion

3.1. The Effect of Temperature on the Formation of the TiO_2 Nanoparticles

The effect of temperature on the formation of the TiO_2 nanoparticles was determined by performing the gel-sol reaction at different temperatures. The XRD results of the synthesized TiO_2 showed that all the samples exhibited only the rutile crystal structure. Since the XRD did not show any distinctive differences between the samples, not even regarding the crystallite size as calculated by the Scherrer equation, a SEM analysis was also performed. This SEM analysis was used to compare the particle sizes and the morphologies of the TiO_2 nanoparticles.

As we can see from Figure 1 the temperature variation of the reaction medium does not have a significant effect on either the particle size or the morphology. This

suggests that other reaction parameters have a greater effect. It is possible that the reaction temperature mostly influences the reaction kinetics, since it is well known that a higher reaction temperature accelerates the progress of the reaction because of the activation energy of the molecules in the reaction medium is attained more rapidly.

3.2. The Effect of Precursor Concentration on the TiO_2 Nanoparticle Formation and the Nucleation Mechanism

Precursor concentration in the reaction medium is one of the most important reaction parameters since it determines the supersaturation and therefore the final-product particle size, as stated in the Becher-Döring nucleation model.¹² Supersaturation is a well-known thermodynamic parameter that determines the change in the Gibbs free energy of the system when the particles begin to form. Depending on the change in the Gibbs free energy the critical size of the nucleus of the growing particle is determined: the bigger the change in the Gibbs free energy, the smaller the critical size of a stable nucleus. Consequently, more nuclei are formed and the final particles are smaller. Therefore, with a substantial supersaturation of the precursor, more nuclei are formed. Since the amount of precursor during particle growth is limited, the number of present nuclei directly determines the size of the particles at the end of reaction. This is one of the most important mechanisms that directly influence the particle size of the product simply by setting and changing the precursor concentration.¹³

According to this theory, we expected that a variation of the precursor concentration would directly affect the final particle size of the rutile. But in our experiments we found that almost no change occurred in the size of the TiO_2 nanoparticles. The particles exhibited the same morphology and a very similar size as shown in Figure 2.

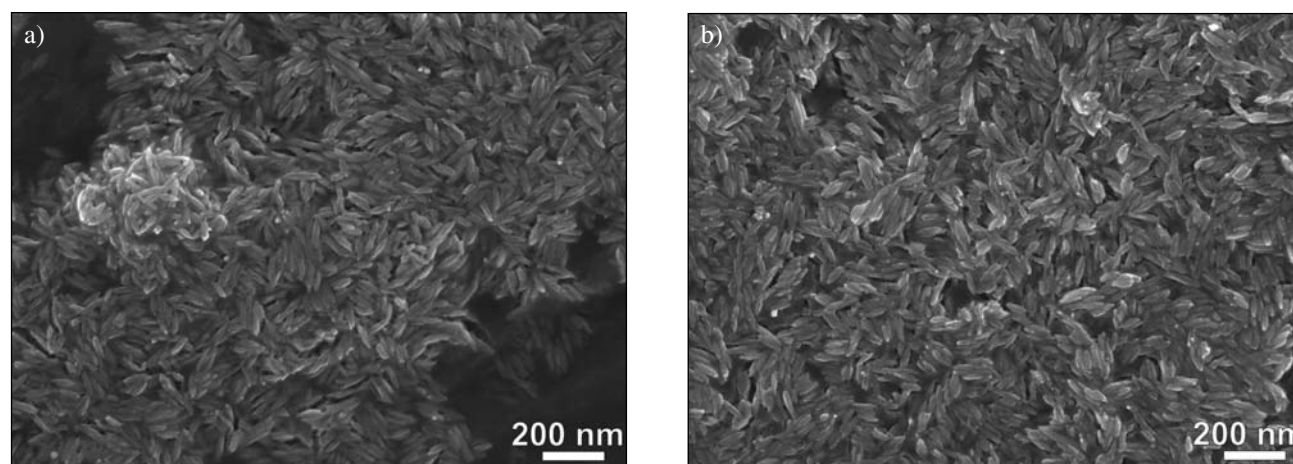


Figure 1. SEM image of rutile nanoparticles synthesized at 50 °C (a) and at 100 °C (b). Both, the mineral acid (HCl) mass concentration and precursor mass concentration were held constant at 70 g/L and 120 g/L, respectively.

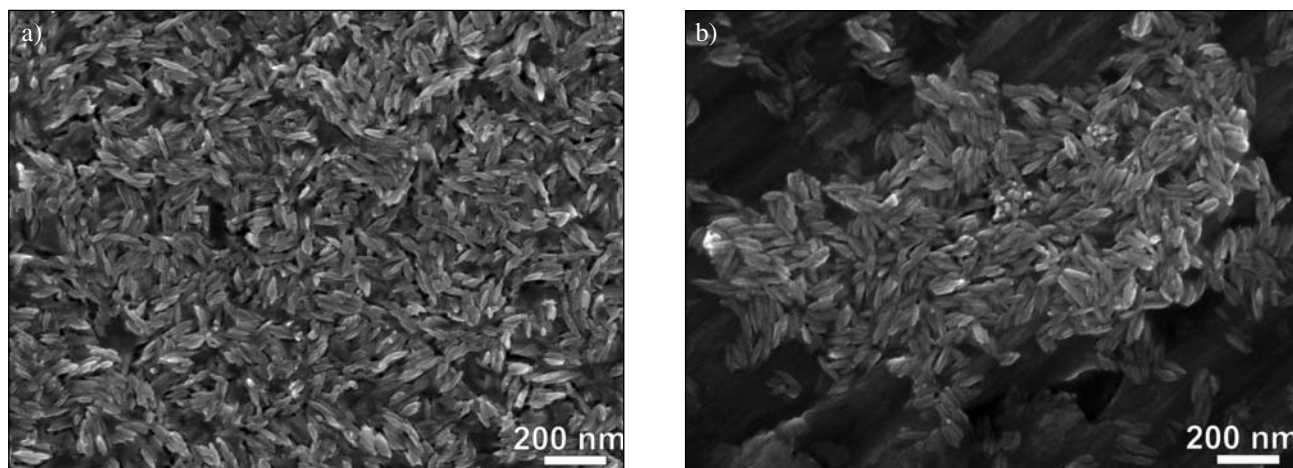


Figure 2. SEM image of rutile nanoparticles prepared at precursor concentrations of 60 g/L (a) and 180 g/L (b). Both, the mineral acid concentration and the reaction temperature were held constant. The mineral acid (HCl) mass concentration was 70 g/L and the reaction temperature was 80 °C.

This result disagrees with the expected difference in the particle size because of the difference in the precursor concentrations. It seems that the underlying mechanism of nucleation in our case was different from the predictions of the Becher-Döring model. The classic nucleation model is based on three assumptions.¹⁴ One of the assumptions is that the supply rate of the solute is independent of the nucleation and growth events. This means that the amount of solute and its consumption during the reaction are not in equilibrium. In this case a monodispersed system is only possible when both the nucleation stage and the growth stage are separated, as proposed in the Lamer-Dinegar model.¹⁴ With the gel-sol system, the above-stated assumption is not true. As was already previously mentioned, the gel-sol synthesis of monodispersed nanoparticles is based on the phase transformation of a highly condensed, metal hydroxide gel or some other gel-like precursor into a sol. The gel acts as a reservoir for the growing particles during its dissolution, which is normally fast enough to be virtually in equilibrium with the consumption rate of the metal ion within the gel throughout the phase-transformation process. Therefore, the supersaturation is not lowered below the nucleation level. Consequently, the nuclei continue to generate and grow. The nuclei form in parallel with the growth process until the precursor gel is completely dissolved. In this case it becomes more difficult to explain how it is possible that the final rutile nanoparticles exhibit such a narrow size distribution. According to Sugimoto¹⁴ the explanation for the observed state is assigned to a possible reduction of the supersaturation with the stabilization of the gel network, which leads to the separation between nucleation and growth. This leads to the formation of a monodispersed system of rutile nanoparticles. Since this explanation is based on aging experiments of the $\text{Ti}(\text{OH})_4$ hydroxide gel, the same assumption may not be strictly applicable in our ca-

se. As was already stated, the rutile nanoparticles form in a reaction between the precursor gel and an appropriate acid. The reactions are therefore different to those that occur during the aging of the gel. A reasonable explanation could be that the particles become monodispersed via two, interconnected processes, namely the formation of primary particles (singlets) that aggregate into secondary particles with a narrow size distribution.¹⁵

It is possible that initially the primary particles form via a burst nucleation, but because of the conditions in the reaction medium they aggregate irreversibly and form the final rutile particles. The conditions that lead to the formation of the secondary (final) particles are determined by the composition of the reaction medium and have a direct impact on the physical characteristics of primary particles such as the surface charge. It is possible that after the burst nucleation in which the primary (monocrystalline) particles form they aggregate into secondary (polycrystalline) nanoparticles due to changes in their surface charge that approaches the isoelectric point when the primary particles achieve a sufficient size. This is in accordance with the observed results. We observed that the underlying structure of the rutile nanoparticles consists of rod-like monocrystalline particles that are irreversibly connected into rutile polycrystalline particles.

Since the isoelectric point directly depends on the pH and/or ionic strength of the reaction medium, the model was tested by changing the medium's chemical composition.

3. 3. The Effect of the Mineral Acid Type on TiO_2 Nanoparticle Formation

The synthesis conditions and the characteristics of the synthesized TiO_2 nanoparticles (particle size, morphology and crystal structure) are given in the Table 1.

Table 2. Summary of the results for the gel-sol synthesis of TiO₂ nanoparticles using sodium titanate as the precursor. The results provided in Table 1 are based on synthesis reactions where the mineral acid type and acid concentration have been changed.

Mineral Acid / Ionic Salt /final mass concentrations (g/L)	Crystal Structure	Particle Size (Length/Width) / nm	Particle Morphology
HCl – 40 g/L	A + R	ND	Poorly defined
HCl – 50 g/L	A + R	ND	Poorly defined
HCl – 60 g/L	A + R	ND	Poorly defined
HCl – 70 g/L	R	~ 80 / ~ 20–30	Anisotropic
HCl – 100 g/L	R	~ 80–90 / ~ 25–30	Anisotropic
HCl – 130 g/L	R	~ 110–130 / ~ 25–30	Anisotropic
HCl – 160 g/L	R	~ 150–160 / ~ 30–40	Anisotropic
HCl – 70 g/L + 25 g/L NaCl	R	~ 80 / ~ 20–30	Anisotropic
HCl – 70 g/L + 50 g/L NaCl	R	~ 70 / ~ 20–25	Anisotropic
HCl – 70 g/L + 100 g/L NaCl	R	~ 65–75 / ~ 15–20	Anisotropic
HNO ₃ – 70 g/L	A + R	ND	Poorly defined
HNO ₃ – 130 g/L	R	~ 80 / ~ 15–20	Anisotropic
H ₂ SO ₄ – 100 g/L	A	ND	Poorly defined
H ₂ SO ₄ – 200 g/L	A	ND	Poorly defined
H ₂ SO ₄ – 300 g/L	A	ND	Poorly defined
H ₂ SO ₄ – 400 g/L	A	ND	Poorly defined

(A – anatase, R – rutile, ND – not determined)

The gel-sol synthesis was first conducted with hydrochloric acid. The X-ray diffraction analysis revealed that the hydrochloric acid concentration directly influences the crystal structure of the TiO₂ product. Namely, it was observed that pure rutile was formed only when the acid concentration was greater than 70 g/L. If the acid concentration was kept below 70 g/L, a mixed product of both anatase and rutile was obtained (Figure 3).

This effect could be a consequence of the precursor sodium titanate's structure, in which the [TiO₆] octahedra arrangement resembles very closely the arrangement of [TiO₆] octahedra in anatase.¹⁶ The acid leads to the rear-

range of the [TiO₆] octahedra present in the sodium titanate structure. Depending on the HCl concentration, the rearrangement of the octahedra can result either in anatase or rutile, or a mixture of both. Clearly, the rearrangement mechanism must be different for the two TiO₂ polymorphs since they differ in the crystal structure and since in our experiments rutile TiO₂, as well as mixed TiO₂ products (rutile/anatase), were produced.

The anatase crystal structure can be viewed as a zig-zag chain of octahedra, linked to each other through shared edges. The rutile crystal structure, on the other hand, is formed by sharing two opposing octahedra edges, crea-

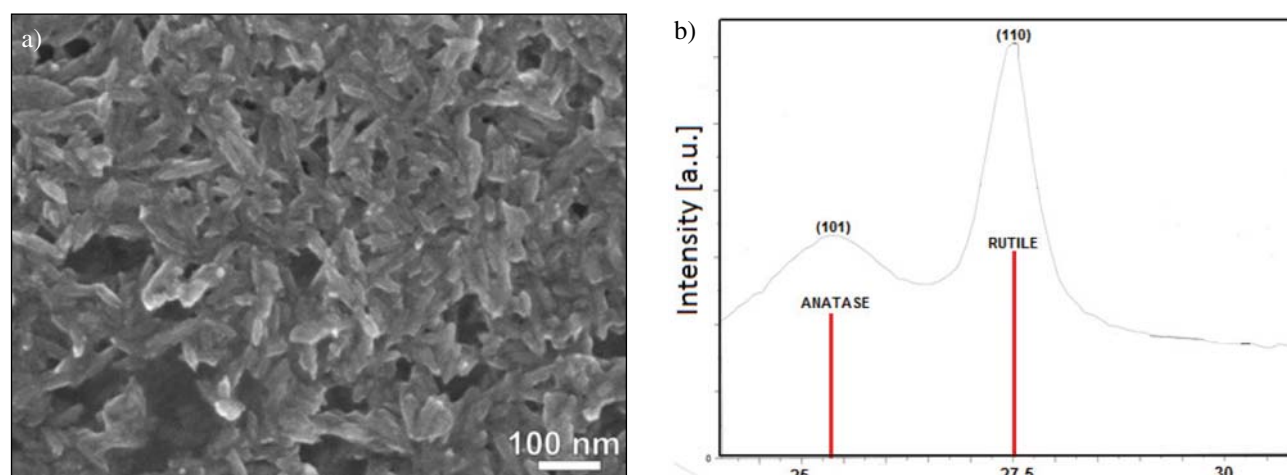


Figure 3. SEM image and XRD diffractogram of A/R mixed product prepared when the HCl acid concentration was lower than needed for the total conversion of the precursor gel into rutile nanoparticles. a) SEM image of A/R mixed product having no distinctive particle morphology. b) X-ray powder diffractogram of the mixed phase product showing the most distinctive peaks for anatase (101) and rutile (110), respectively.

ting linear chains along. [001]¹⁷ Some anatase was produced, but only when the HCl acid concentration during the gel-sol synthesis was lower than 70 g/L. In this case the acid could only act to remove the interlayer ions present in the titanate precursor, which would lead to the merging of the octahedra layers. Since the octahedra arrangement within the titanate layers is similar to the octahedra arrangement in the anatase crystal structure, the merging of the layers leads to the formation of anatase.¹⁶ When the acid concentration was equal to or more than 70 g/L, only rutile particles were produced as seen in Figure 4.

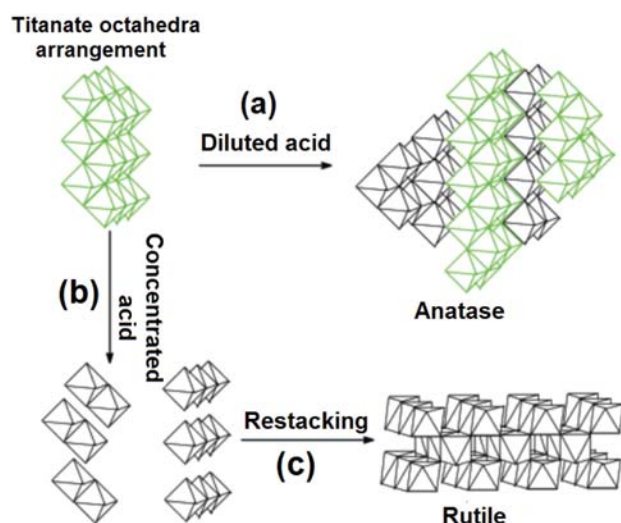


Figure 4. A schematic representation of a possible phase transition between the titanate material and the anatase and rutile TiO_2 crystal structures [16]. (a) If a diluted HCl is used, the $[\text{TiO}_6]$ octahedra layers of the titanate merge and form particles with the anatase crystal structure. (b) – (c) When concentrated HCl is used, the titanate dissolves and the $[\text{TiO}_6]$ octahedra restack into particles with the rutile crystal structure.

Since the rutile crystal structure differs in the $[\text{TiO}_6]$ octahedra arrangement, compared to the arrangement of the $[\text{TiO}_6]$ octahedra in sodium titanate, the rearrangement mechanism should begin with deoxolation reactions that lead to the detachment of the octahedra in the titanate precursor.¹⁸ Deoxolation could start with the advance of the electrophilic protons on the oxygen bridges between the titanium ions. This results in a lowered electron density of the latter and makes it more electrophilic, which leads to the attraction of the titanium ions with the chloride anions and consequently to the breaking of the oxolation bond. The reduced number of Ti-O-Ti bonds leads to structural rearrangements of the $[\text{TiO}_6]$ octahedra and, consequently, very small rutile particles are formed. This is in accordance with the fact that very acidic environments tend to lead to the formation of rutile.¹⁹

The distinction between the $[\text{TiO}_6]$ rearrangement mechanisms between anatase and rutile becomes even more evident when analyzing the morphology of the pro-

duced particles. When the HCl acid concentration was low, both anatase and rutile formed. The TEM analysis revealed that rutile was produced in the form of very small anisotropic nanoparticles consisting of rod-like crystallites. On the other hand, anatase was produced in the form of larger aggregates consisting of very small crystallites, about 5 nm in size. The difference in the constituent crystallite size and the particle morphology between the rutile and anatase phases is only possible when the particle-formation mechanisms differ. Anatase is present in the form of large aggregates, which is consistent with the fact that a deoxolation reaction does not occur (Figure 4), and therefore the initial titanate precursor is not broken down. In order that the rutile particles form, deoxolation must occur, since only then the $[\text{TiO}_6]$ octahedra within the titanate precursor split and can rearrange into the rutile crystal structure. The morphology of the crystallites that form the rutile nanoparticles is clear evidence for this (Fig. 5).

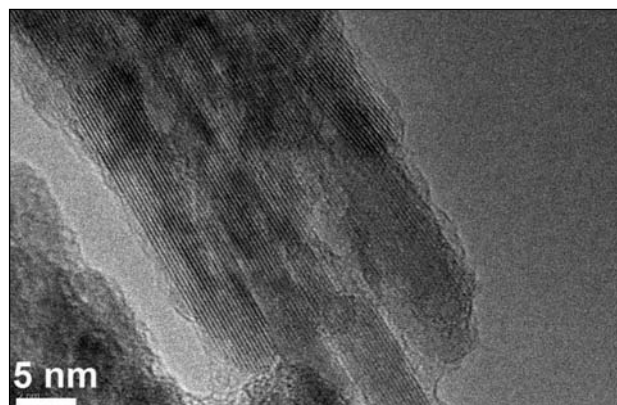


Figure 5. TEM image of a polycrystalline rutile nanoparticle. The constituent crystallites have an anisotropic rod-like morphology.

As is clear from Figure 5 the crystallites that form the rutile nanoparticles exhibit a rod-like anisotropic morphology and have a well-defined structure. Their morphology and crystallinity can be explained via polycondensation reactions starting from the $[\text{TiO}_6]$ octahedra that form in a highly acidic environment. The $[\text{TiO}_6]$ octahedra form because of the deoxolation reactions and the breaking of the Ti-O-Ti bonds. The $[\text{TiO}_6]$ octahedra act as building blocks for the newly formed rutile particles. The anisotropic morphology of the rutile nanoparticles is a direct result of a specific $[\text{TiO}_6]$ octahedra rearrangement and polycondensation reactions that take place on newly formed rutile nuclei. The rutile crystal structure is tetragonal. Therefore, the surface energies of the individual rutile crystal facets differ.²⁰ The difference in surface energies can lead to selective adsorption of the species present in the reaction medium. The $[\text{TiO}_6]$ octahedra and chloride anions can both adsorb on the surface of the growing rutile crystal. Since the crystal facets of rutile differ in their energies, the adsorption of the two species is different for a specific facet.

Depending on the adsorption ratio of the $[\text{TiO}_6]$ octahedra and the chloride anions on a specific rutile facet the crystal growth becomes anisotropic. Consequently, the rutile crystal grows faster in the $\{101\}$ direction since a higher ratio of $[\text{TiO}_6]$ octahedra is adsorbed.²⁰ This leads to an anisotropic crystal morphology, as seen on the high-resolution TEM (HRTEM) image in Figure 5. Eventually, the crystallites aggregate and form the final rutile nanoparticles. The rutile nanoparticles are of different sizes, based on the hydrochloric acid concentration used.

This is probably because of the specific conditions present in the reaction medium, which are determined by the type of ions present and their concentration. We speculate that during the growth of the crystallites their properties (i.e., surface charge) change. At a certain crystallite size the isoelectric point is attained and at this point the irreversible aggregation of the crystallites occurs and the final rutile nanoparticles form. This hypothesis was tested by performing the synthesis reactions with higher HCl acid concentrations. We assume that in such conditions the sur-

face charge of the growing particles is different compared to the surface charge at lower HCl acid concentrations because the particle's electrical double layer is directly affected by the chemical composition of the reaction medium. A possible consequence is that the crystallites and rutile nanoparticles become different in size since the isoelectric point during the crystallite growth is attained at different stages. This is supported by our SEM analysis of the rutile nanoparticles that were synthesized with various HCl acid concentrations (Figure 6).

From the SEM micrographs in Figure 6 it is clear that when performing the gel-sol reaction with a higher hydrochloric acid concentration, the rutile nanoparticles become larger. This can mainly be attributed to the difference in the reaction medium's chemical composition, which differs mostly in terms of the ionic strength. The ions present in the medium constitute the electrical double layer of the colloid particles and to a large extent determine their physical properties, such as stability, surface charge, etc. Changing the ionic strength of the medium di-

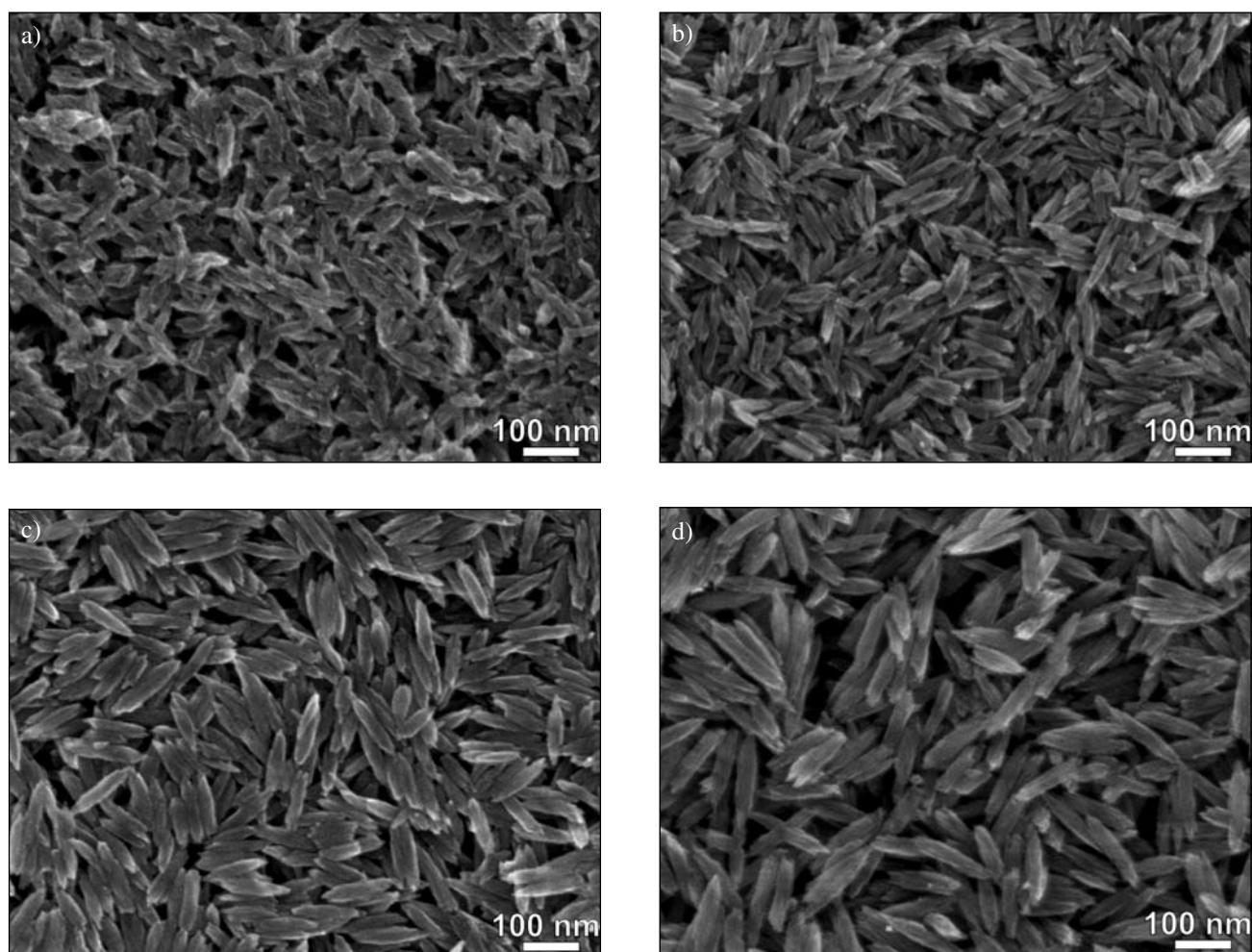


Figure 6. SEM images of rutile nanoparticles that were synthesized using various hydrochloric acid concentrations. The rutile nanoparticles were synthesized with the following HCl concentrations: 70 g/L (a), 100 g/L (b), 130 g/L (c) and 160 g/L (d).

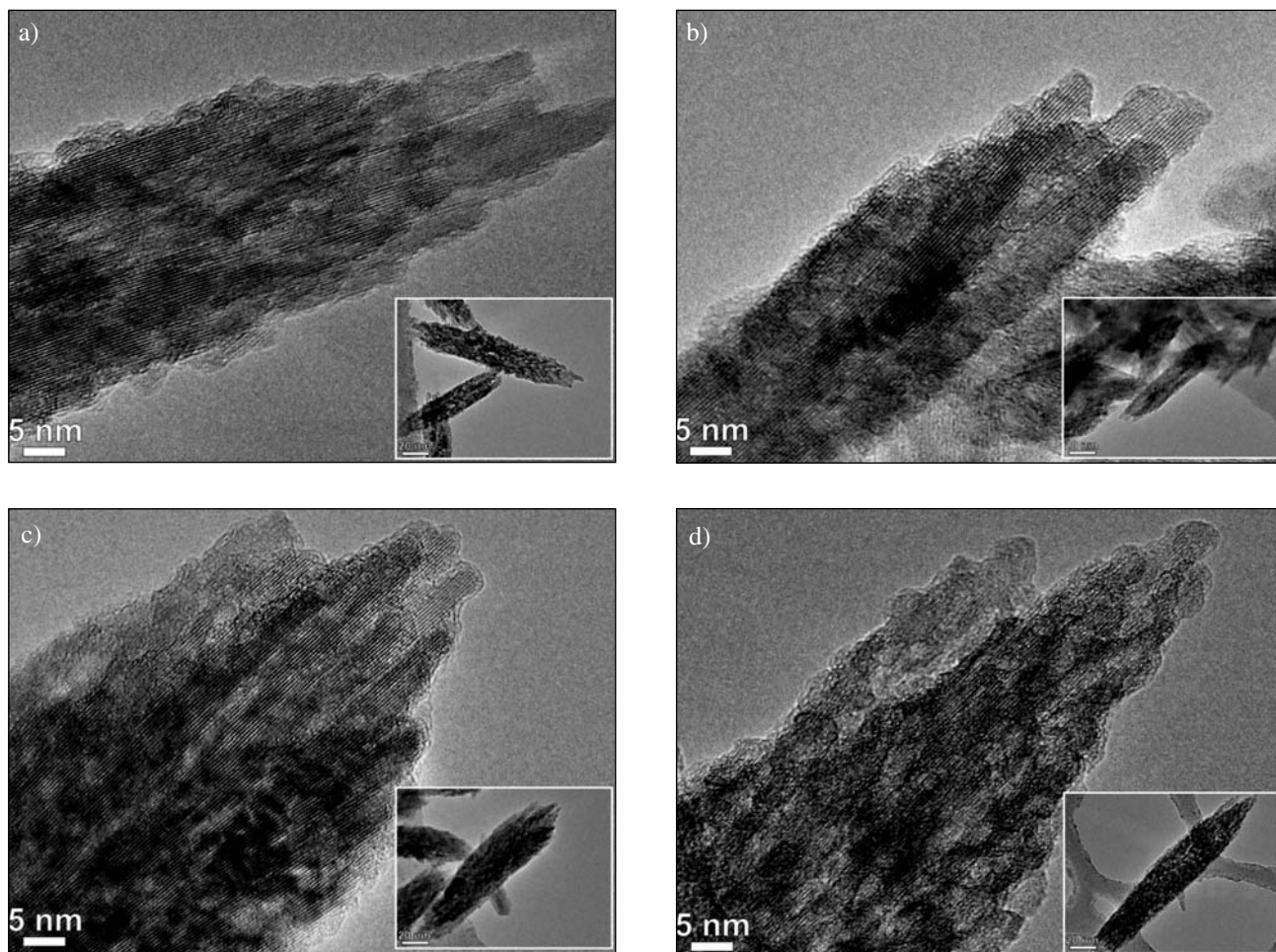


Figure 7. TEM images of rutile nanoparticles prepared with gel-sol synthesis using various HCl concentrations. The HCl acid concentrations were (a) 70 g/L, (b) 100 g/L, (c) 130 g/L and, (d) 160 g/L. The nanoparticles are composed of crystallites with a rod-like morphology. The crystallites are anisotropic and differ slightly in length, while their width is about the same (~4–5 nm). The inset scale bar represents 20 nm in length.

rectly changes the electrical double layer of the growing colloid rutile particle, which as a result affects the isoelectric point. Consequently, the irreversible aggregation of rod-like crystallites into the final rutile particles happens at different stages. This leads to the formation of rutile nanoparticles with different sizes.

In order to additionally elucidate the effect of the reaction medium's composition on the structure and size of rod-like crystallites that aggregate into the final rutile nanoparticles, a HRTEM analysis was employed (Figure 7).

Fig. 7 shows that the increased acid concentration directly affects the size of the rod-like crystallites and nanoparticle as a whole. The rod-like crystallites grow in length when the acid concentration is increased, while the width stays about the same. This is in accordance with the above-proposed crystallite aggregation model that is directly dependent on the ionic strength of the reaction medium. The ionic strength of the reaction medium is mainly affected by the HCl concentration used during the synthesis. Therefore, when the HCl concentration is increased, the aggregation of the crystallites occurs at a different sta-

ge than when the HCl concentration is lower. The rod-like crystallites can therefore grow for a longer period of time at a higher HCl concentration, which increases their length and the length of the rutile nanoparticle as a whole. The XRD results support these assumptions. But it must be taken into account that the crystallite size as provided by the Scherrer equation calculation gives only an average value of crystallite size dimensions. So, the larger crystallite size as observed by XRD can be attributed to longer crystallites {101} direction because the final particles become larger due to a higher hydrochloric acid concentration (see Table 2). The question remains whether the crystallites become also wider in size. This, however, cannot be analyzed using XRD, it can only be estimated by TEM analysis. Upon inspecting Figure 7 in more detail it is our assumption that the crystallites do not significantly differ in their respective width, although they significantly differ in their respective length.

The effect of the chemical composition (ionic strength) of the reaction medium on the nanoparticle size was further tested by performing experiments in which an

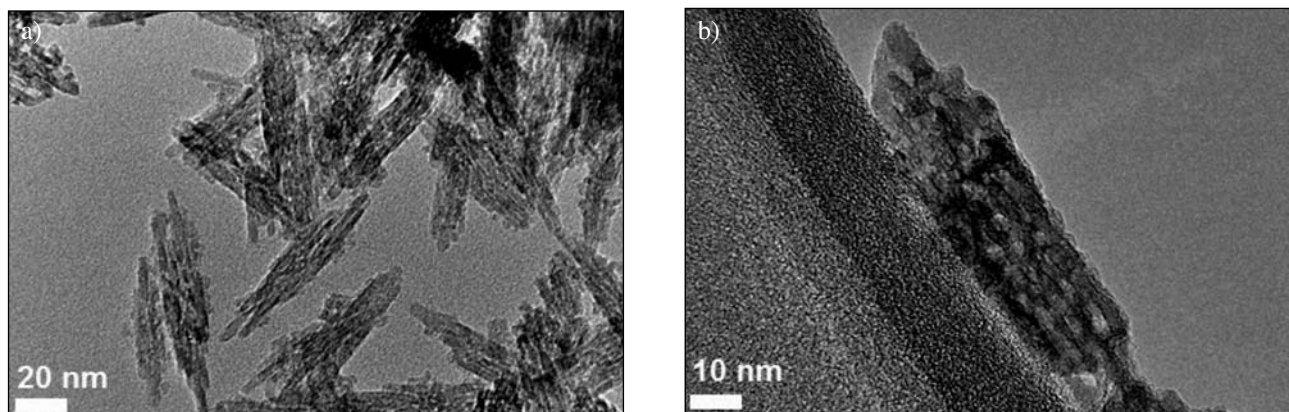


Figure 8. Low-magnification and HRTEM of rutile nanoparticles prepared at a 70 g/L HCl concentration and NaCl (100 g/L). (a) TEM images of rutile nanoparticles acquired by adding sodium chloride into the reaction medium. (b) HRTEM of a rutile nanoparticle prepared with gel-sol synthesis where the acid concentration was 70 g/L and the reaction medium also contained NaCl.

ionic salt was added. The added ionic salt was sodium chloride, since it has already been established that sodium cations may affect the size of TiO_2 particles during their formation.^{20–22}

As one can see from Figure 8, the rutile nanoparticles synthesized in the presence of sodium chloride are smaller than those obtained in a reaction performed only with HCl. It seems that hydrochloric acid, its concentra-

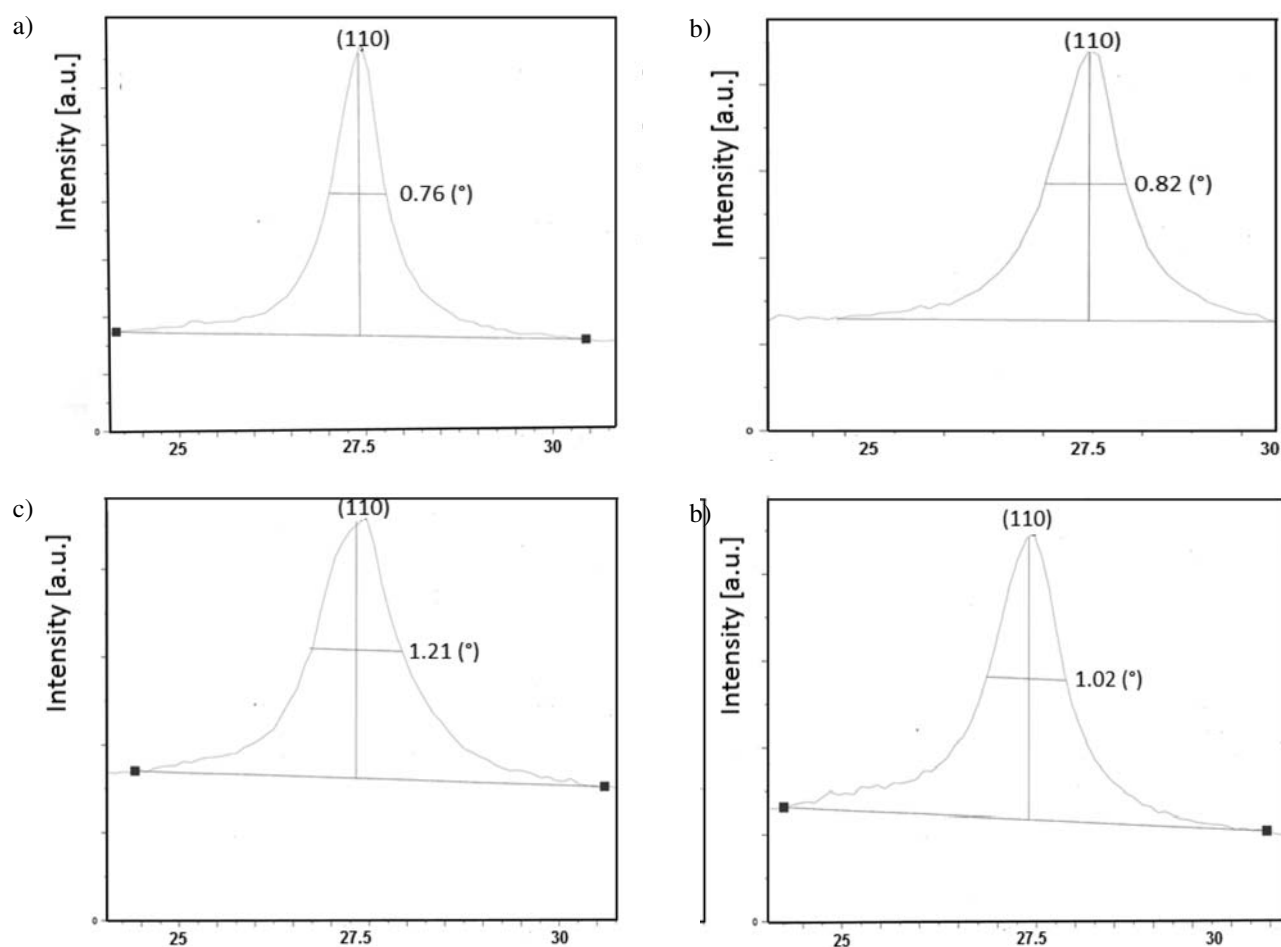


Figure 9. XRD diffractograms showing the representative peak (110) of rutile nanoparticles prepared at constant HCl mass concentration (70 g/L) and various NaCl mass concentrations ranging from a) 0 g/L, b) 25 g/L, c) 50 g/L and d) 100 g/L.

tion and also the presence of other ionic species have the most profound effect on the produced TiO_2 nanoparticles.

Again, the XRD analysis results of the samples prepared using sodium chloride when the HCl mass concentration was kept constant (70 g/L) show that based on the final mass concentration of NaCl, the respective crystallite sizes differ as seen in Figure 9.

As one can see from Figure 9, the XRD diffractograms differ, which can be attributed to the difference in sodium chloride mass concentration in respective samples. The width of the (110) peaks differ, which means that the average crystallite sizes also differ. The change in the individual crystallite sizes of the rutile samples can be attributed to the difference in the length of the final particles (see Table 2). However, any change in the crystallite width cannot be elucidated using the XRD crystallite size calculation based on Scherrer equation. Nevertheless, it seems reasonable to assume that both, length and width of individual crystallites varies when the change in the composition of the reaction medium is significant.

Based on these results it was reasonable to carry out the also some experiments with other mineral acids, such as nitric acid (HNO_3) and sulfuric acid (H_2SO_4), in order to further elucidate the above-stated mechanism of the precursor transformation into rutile.

When the nitric acid concentration was 130 g/L the XRD results showed that the product synthesized was pure rutile. When the nitric acid concentration was 70 g/L a mixture of rutile and anatase was formed. The presence of both polymorphs at a 70 g/L nitric acid concentration can be explained in the following way. The driving mechanism for the titanate precursor's transformation into rutile is driven solely on the basis of the molar ratio between the precursor and the acid. If the molar ratio between the acid protons (H^+) and the precursor Ti^{4+} ions is too low, a mixture of anatase and rutile is formed. This is because the sodium titanate $[\text{TiO}_6]$ octahedra rearrange via two competi-

tive mechanisms shown in Figure 4 (a) and (b). One leads to rutile particle formation and the other to anatase particle formation. When the synthesis was carried out with a nitric acid concentration of 130 g/L the product was pure rutile, which is reasonable since the H^+ molar concentration is about the same as with a hydrochloric acid concentration of 70 g/L, which also leads to the formation of pure rutile. The experiments carried out using nitric acid confirmed that the acid and its concentration drive the precursor transformation into either rutile or a mixture of rutile and anatase. In order to compare the TiO_2 produced with nitric acid and hydrochloric acid a SEM analysis was performed (Figure 10).

As is clear from Figure 10, the produced nanoparticles exhibit a very similar morphology and particle size to those produced with hydrochloric acid. This probably means that a nitrate anion behaves similarly to a chloride ion in the sense that they both have an extra electron (they act as a Lewis base), which makes it possible to bind electrostatically to areas of lower electron density. Therefore, the nitrate anion could bind onto the surface of a growing rutile particle like the chloride anion does, which leads to anisotropic crystallite growth and particle morphology. This is a confirmation of the results already acquired, namely that the acid concentration determines the final product's crystal structure and particle size, while the anion present determines the particle morphology.

Since sulfuric acid is a strong mineral acid it could also cause rutile formation when added in large amounts. However, the XRD analysis of the TiO_2 materials synthesized when sulfuric acid was used showed that only anatase is formed, regardless of the sulfuric acid concentration in the reaction medium. This means that sulfate anions exhibit an effect that dominantly directs the transformation of the titanate precursor into anatase only. The reason for this observation is that the sulfate anions prevent the $[\text{TiO}_6]$ octahedra from rearranging into linear chains that are specific

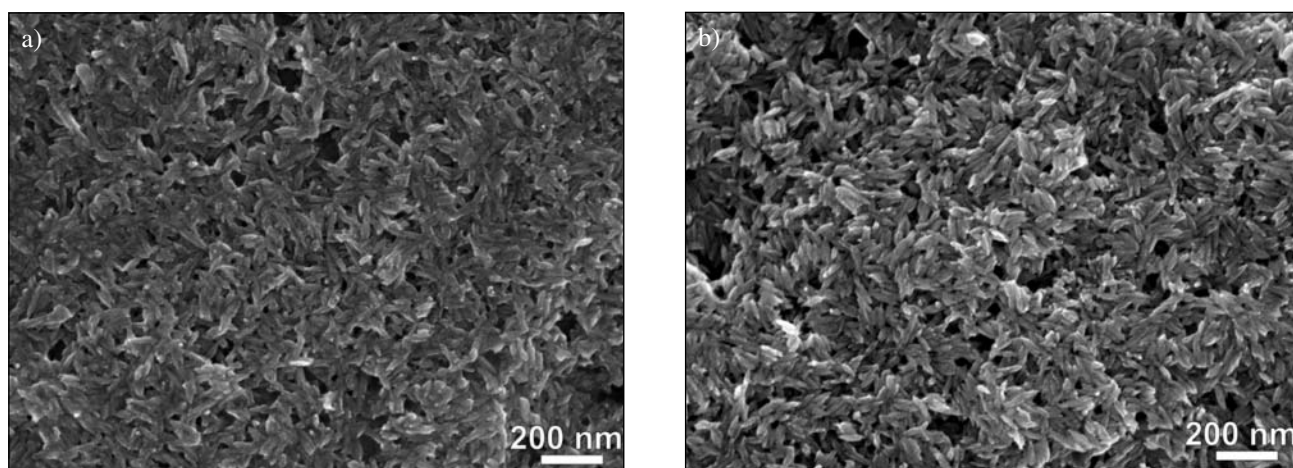


Figure 10. SEM images of nanoparticles produced with nitric acid at different concentrations. The nitric acid concentration was 70 g/L (a) and 130 g/L (b).

to the rutile crystal structure.²³ Only zig-zag $[\text{TiO}_6]$ octahedra chains form, as schematically presented in Figure 11. This leads to the formation of anatase particles.

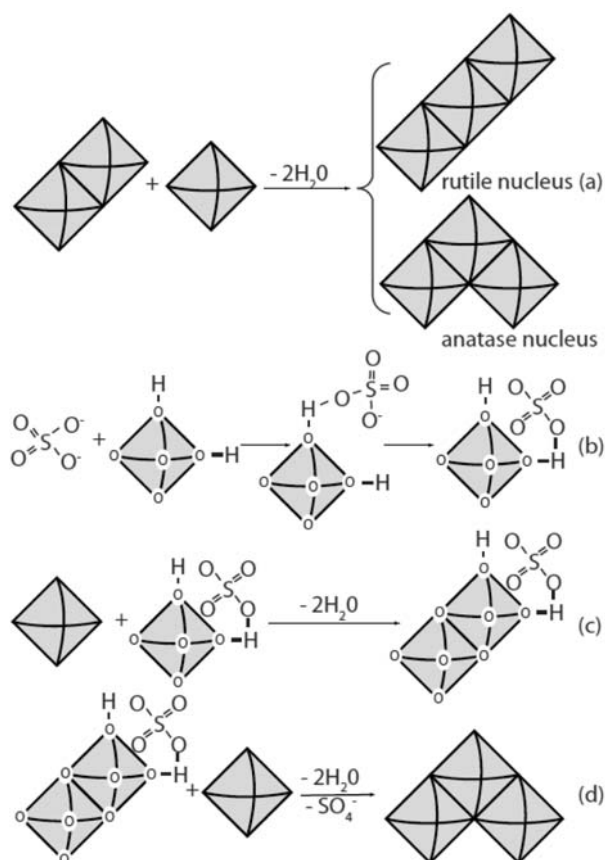


Figure 11. A scheme of possible precursor transformations into anatase when a sulfate ion is present in the reaction medium. (a) The TiO_6 octahedra arrangement determines whether a rutile or an anatase nucleus will be formed. (b) The sulfate ion interacts with the TiO_6 octahedra hydroxyl groups. (c) Two TiO_6 octahedra share an edge in the presence of the sulfate ion and form a dimer. (d) The third TiO_6 octahedra can bind to the dimer only on the side edge by which an anatase nuclei forms.²³

As seen in Fig. 11 the sulfate ion determines the TiO_2 crystal structure on the basis of absorption onto TiO_6 octahedra. This provides a steric hindrance, making it virtually impossible for rutile nuclei/particles with linear chains of TiO_6 octahedra to form.

4. Conclusions

We have developed a simple gel-sol method for the synthesis of rutile nanoparticles. By changing the selected processing parameters (temperature, TiO_2 precursor concentration, acid type and concentration) we were able to produce rutile nanoparticles with defined sizes that can be

used in various technological applications. Our results showed that the choice of mineral acid and its concentration have the most profound effect on the rutile particle size. In the case of HCl we were able to repeatedly control the size of the rutile nanoparticles within a size range from 60 to 160 nm by changing the acid concentration. Furthermore, based on our systematic study of the influence of the experimental parameters on the rutile nanoparticles, we propose a possible nucleation/growth model that explains the polycrystalline nature of the rutile nanoparticles.

5. Acknowledgment

This work is partially financed by the European Union, European Social Fund and is based in part on the Ph.D. thesis of Dejan Verhovšek under Grant P-MR-07/26 by the TIA of Republic of Slovenia. The authors would also like to greatly acknowledge Cinkarna Celje Inc., which provided the raw material needed to perform the research presented in this paper. The electron microscopy was performed at the Center for Electron microscopy at the Jožef Stefan Institute.

6. References

- Linsebigler, A. L.; Guangquan, L.; Yates, J. T. Jr. Photocatalysis on TiO_2 Surfaces: Principles, Mechanisms, and Selected Results *Chemical Reviews* **1995**, *95*, 735–758.
- Zhang, Z.; Wang, C. C.; Zakaria, R.; Ying, J. Role of Particle Size in Nanocrystalline TiO_2 -Based Photocatalysts. *Journal of Physical Chemistry B* **1998**, *102*, 10871–10878.
- O'Regan, B.; Gratzel, M. A low-cost, high-efficiency solar cell based on dye-sensitized colloidal TiO_2 films. *Nature* **1991**, *353*, 737–740.
- Georg, A.; Opara Krašovec, U.; Photoelectrochromic window with Pt catalyst. *Thin Solid Films* **2006**, *502*, 246–251.
- Kumar, K. N. P.; Keizer, K.; Burggraaf, A. Densification of nanostructured titania assisted by a phase transformation. *Nature* **1992**, *358*, 48–51.
- Park, H. K.; Kim, D. K.; Kim, C. H. Effect of Solvent on Titania Particle Formation and Morphology in Thermal Hydrolysis of TiCl_4 . *Journal of the American Ceramic Society* **1998**, *80*, 743–749.
- Manuel, O.; Josev, G. R.; Carlos, S. Low-Temperature Nucleation of Rutile Observed by Raman Spectroscopy during Crystallization of TiO_2 . *Journal of the American Ceramic Society* **1992**, *75*, 2010–2012.
- Cheng, H.; Ma, J.; Zhao, Z.; Qi, L. Hydrothermal Preparation of Uniform Nanosize Rutile and Anatase Particles. *Chemistry of Materials* **1995**, *7*, 663–671.
- Park, N. G.; Schlichthorl, G.; van de Lagemaat, J. Dye-Sensitized TiO_2 Solar Cells: Structural and Photoelectrochemical Characterization of Nanocrystalline Electrodes Formed

- from the Hydrolysis of TiCl_4 . *Journal of Physical Chemistry B* **1999**, *103*, 3308–3314.
10. Aruna, S. T.; Tirosh, S.; Zaban, A. Nanosize rutile titania particle synthesis via a hydrothermal method without mineralizers. *Journal of Materials Chemistry* **2000**, *10*, 2388–2391.
 11. Sugimoto, T.; Zhou, X.; Muramatsu, A. Synthesis of uniform anatase TiO_2 nanoparticles by gel-sol method. 3. Formation process and size control. *Journal of Colloid and Interface Science* **2003**, *259*, 43–52.
 12. Becher, R.; Döring, W. Kinetische Behandlung der Keimbildung in übersättigten Dämpfen. *Annalen der Physik* **1935**, *416*, 719–752.
 13. Guozhong, C. *Nanostructures & Nanomaterials – Synthesis, properties and applications*. (Imperial College Press, London, 2004).
 14. Sugimoto, T. Underlying mechanisms in size control of uniform nanoparticles. **2007**, *309*, 106–118.
 15. Park, J.; Privman, V.; Matijević, E. Model of formation of monodispersed colloids. *Journal of Physical Chemistry B* **2001**, *105*, 11630–11635.
 16. Zhu, H. Y.; Lan, X.; Gao, X. P.; Ringer, S. P.; Zheng, Z. F.; Song, D. Y.; Zhao, J. C. Phase Transition between Nanostructures of Titanate and Titanium Dioxides via Simple Wet-Chemical Reactions. *Journal of the American Chemical Society* **2005**, *127*, 6730–6736.
 17. Li, Y.; White, T.J.; Lim, S.H. Low-temperature synthesis and microstructural control of titania nano-particles. *Journal of Solid State Chemistry* **2004**, *177*, 1372–1381.
 18. Zhang, R.; Gao, L. Effect of peptization on phase transformation of TiO_2 nanoparticles. *Materials Research Bulletin* **2001**, *36*, 1957–1965.
 19. Madhusudan, R. K.; Guin, D.; Manomara, S.V. Selective synthesis of nanosized TiO_2 by hydrothermal route: Characterization, structure property relation, and photochemical application. *Journal of Materials Research* **2004**, *19*, 2567–2575.
 20. Zhang, Q.; Gao, L. Preparation of Oxide Nanocrystals with Tunable Morphologies by the Moderate Hydrothermal Method: Insights from Rutile TiO_2 . *Langmuir* **2003**, *19*, 967–971.
 21. Koelsch, M.; Cassignon, S.; Jolivet, J. P. Synthesis of nanometric TiO_2 in aqueous solution by soft chemistry: obtaining of anatase, brookite and rutile with controlled shapes. *Materials Research Society Symposium Proceedings*, **2004**, *822*, S.5.3.1-S5.3.6.
 22. Huang, Q.; Gao, L. A Simple Route for the Synthesis of Rutile TiO_2 Nanorods. *Chemistry Letters* **2003**, *32*, 638–639.
 23. Shi, L. J.; Yang, R.; Li, M. Nanocrystalline TiO_2 : Crystal Structure Controlled Synthesis via Low Temperature Hydrolysis Method and Surface Texture. *Chinese Journal of Inorganic Chemistry*, **2006**, *22*, 1196–1202.

Povzetek

V članku poročamo o sol-gel sintezi nanodelcev titanovega dioksida (TiO_2) s kristalno strukturo rutila pri temperaturah pod $100\text{ }^\circ\text{C}$. S spreminjanjem ustreznih procesnih parametrov smo lahko ponovljivo kontrolirali velikost, obliko in kristaliničnost sintetiziranih nanodelcev. Rutilne nanodelce TiO_2 smo analizirali z metodo rentgenske praškove difrakcije (XRD), z vrstično elektronsko mikroskopijo (SEM) in s presevno elektronsko mikroskopijo (TEM). Rezultati analiz so pokazali, da na končne lastnosti nanodelcev TiO_2 najbolj vpliva izbira mineralne kisline in njena koncentracija pri izvedbi reakcije. Z opisano gel-sol metodo in z optimizacijo ustreznih reakcijskih parametrov smo uspeli sintetizirati anizotropne nanodelce rutila z dolžino med 60 in 160 nm in z razmerjem med dolžino ter širino približno 5. Predstavili smo ustrezen reakcijski mehanizem, s katerim smo razložili vpliv različnih reakcijskih parametrov na končne lastnosti nanodelcev TiO_2 .